Quasiclassical approximation for the beamstrahlung process

Andrey V. Solov'yov,* Andreas Schäfer, and Christian Hofmann
Institut für Theoretische Physik der Universität, 6000 Frankfurt am Main, Germany
(Received 19 May 1992)

The beamstrahlung spectrum for colliding electron (positron) bunches is calculated by a quasiclassical method. The derived formulas apply to the classical and the quantum domain of parameters. Scaling laws for the total radiation energy loss and for the photon spectrum are derived. Our numerical results are in good agreement with those of a previous, purely quantum-mechanical calculation.

PACS number(s): 41.75.Ht, 29.20.−c

I. INTRODUCTION

Dense pulses of electrons and positrons, consisting of about 10^{10} particles, are created in the modern colliders. When these pulses pass through one another a considerable portion of their kinetic energy is radiated as photons. This radiative process was called beamstrahlung [1,2]. The interest in beamstrahlung is greatly increased by prospects of building high-energy linear colliders for electron and positron beams in the TeV region. This process must be taken into account in designing such colliders because the energy loss due to beamstrahlung can be considerable. The quantum-mechanical calculation performed in [1,2] predicts approximately 20% fractional energy loss for colliders that are envisaged to be constructed in the near future. We confirm this result in our work, using a quasiclassical method.

This quasiclassical method is based on the following assumptions. The electron or positron, colliding with the dense pulse of the opposite charge, scatters and radiates in the mean field created by all particles of the pulse. This collective phenomenon takes place because the bremsstrahlung coherence length for individual collisions substantially surpasses the interparticle distances in the pulse.

The ultrarelativistic particle radiates into a narrow cone with the opening angle $1/\gamma$ along the direction of motion [3], where γ is the relativistic Lorentz factor. The deflection angle θ_d of the particle crossing the pulse is much larger than the typical radiation angle $\theta_d \gg 1/\gamma$. This condition shows that the radiation in a given direction arises on a small piece of trajectory parallel to this direction. If the angle between two different pieces of trajectory surpasses the radiation angle, then the photons from these pieces of trajectory do not interfere and the corresponding contributions to the total radiation spectrum and the energy loss have simply to be summed. The small pieces of the trajectory, where the particle radiates coherently, can be approximated by a part of a circle. The radiation of the particle, moving through this circle trajectory (synchrotron radiation) is very well known (see, e.g., [3,4]). This radiation is described by the quasiclassical method, which is valid both in the classical and in the quantum limits. The quantum behavior appears when the frequency of the emitted photon is about the energy of the projectile particle. Using the intensity of synchrotron radiation derived by the quasiclassical method at each moment of time and integrating it over the particle's trajectory in the pulse, we obtain the total energy loss and the spectrum of the emitted photons. These characteristics have to be averaged over all possible trajectories. The results of our calculations are in a good agreement with those that have been derived in a pure quantum treatment of beamstrahlung [1,2].

The wave function of the projectile in the quantum treatment was derived assuming a uniform charge distribution of the pulse [1,2]. The influence of the pulse geometry on the beamstrahlung process was also investigated [5–7] and various charge distributions have been considered.

In our treatment, the electric field of the bunch acting on the projectile particle is considered as being produced by a uniform and cylindrically symmetrical charge distribution. The influence of the pulse field on the particle motion is too strong to be described perturbatively. We show that the quasiclassical approximation is appropriate for description of the beamstrahlung process.

The scaling law for the beamstrahlung fractional energy loss was proposed in [1]. The function, describing the deviation from the classical behavior, depends on the scaling parameter

$$C_b = \frac{m^2 c^3 R L}{4 N e^2 \gamma^2} .$$

The scaling parameter is a complicated combination of values characterizing the process. Here c is the velocity of light; m and e are the mass and the charge of the electron; N is the number of particles in the pulse, and L and R are the length and the radius of the pulse. We use in this paper the atomic system of units in which $m = |e| = \hbar = 1$.

The scaling function tends to unity with increasing scaling parameter. This is the classical region. In the quantum limit, the parameter C_b is small and the scaling function tends to zero.

The quasiclassical treatment of beamstrahlung provides a similar scaling behavior of the beamstrahlung fractional energy loss as a function of C_b but the analytical form for the scaling function is different. This function fits the results of quantum treatment of beamstrahlung within several percent accuracy.

We have calculated the total energy loss in the quan-

TABLE I. Sets of parameters characterizing pulses which are available in different colliders.

Parameter	SLC	Super	JLC		
N	5×10^{10}	3×10^{8}	1.1×10^{10}	1.8×10^{10}	2.3×10^{10}
R (Å)	10^4	5	2×10^2	1.6×10^2	1.9×10^2
L (cm)	10^4	3×10^2	1.6×10^4	1.2×10^4	2.9×10^4
γ	10^5	10^7	10^6	2×10^6	2.9×10^6
$l=L\gamma^{-1}$ (cm)	10^{-1}	3×10^{-5}	1.6×10^{-2}	1.2×10^{-2}	10^{-2}

tum and classical limits and investigated the limiting behavior of the general formulas in both cases. We calculated the photon spectrum and the fractional energy loss for the parameters of the Stanford Linear Collider (SLC) and for the envisaged machines with TeV energies (super case). The parameters characterizing SLC and super cases are taken from [1,2] and presented in Table I. We also considered the set of parameters proposed for the Japan Linear Collider Project (JLC) [8]. This project envisages three different sets of pulse parameters. The pulse in JLC is not cylindrical. Therefore we introduce the effective radius R of the pulse according to

$$R=\left[\frac{\sigma_x\sigma_y}{\pi}\right]^{1/1},$$

where σ_x and σ_y are the sizes of the pulse in the transverse plane, being given in [8].

II. QUASICLASSICAL APPROACH

Let us consider a collision of an electron with a positron pulse in the laboratory frame of reference. The electron of energy ε, having the same absolute value of velocity as the positron pulse, moves in the opposite direction. We assume an idealized positron pulse of cylindrical shape having a uniform distribution of charge. This assumption is based on a comparison of the bremsstrahlung coherence length L_c and the average interparticle distance in the pulse. The longitudinal coherence length L_c characterizes the distances which are important for the bremsstrahlung process. It may be estimated as [3]

$$L_c\sim\frac{1}{q_\parallel}\sim\frac{p}{(mc)^2}, \tag{1}$$

where the minimum longitudinal transferred momentum is

$$q_\parallel=p-p'-k=(\varepsilon^2/c^2-m^2c^2)^{1/2}-(\varepsilon'^2/c^2-m^2c^2)^{1/2}-\omega/c .$$

Here (ε,p) and $(\varepsilon';p')$ are the energy and momentum of the electron in the initial and in the final state; $(\omega;k)$ is the frequency and momentum of the emitted photon. We suppose that $\omega\sim\varepsilon'\sim\varepsilon$. The average interparticle distance in the pulse is equal to

$$D\sim\left[\frac{\pi R^2 l}{N}\right]^{1/3}. \tag{2}$$

The ratio D/L_c is equal to

$$\left[\frac{D}{L_c}\right]_{\rm SLC}=2.2\times10^{-1},\quad \left[\frac{D}{L_c}\right]_{\rm super}=2.4\times10^{-6},$$
$$\left[\frac{D}{L_c}\right]_{\rm JLC}=6.8\times10^{-4}$$

in cases presented in Table I. These estimates show that the inequality $D\ll L_c$ is fulfilled in all cases under consideration. This condition proves that the radiation in the process considered is not a result of successive collisions with single particles, but is generated during motion of the particle in the average electric field. We use the first set of parameters of the JLC.

The transverse extent R of the pulse is substantially smaller than its length L, see Table I. Therefore, neglecting edge effects, one can approximate the electric field of the pulse in its rest frame by the field of the infinitely long and uniformly charged cylinder, which inside the pulse is

$$\mathbf{E}'=\frac{2Ne}{LR^2}\mathbf{r}, \tag{3}$$

where $\mathbf{r}$ is the radius vector in the transverse plane of the pulse.

Performing the Lorentz transformations, one derives from (3) the electric field $\mathbf{E}$ and the magnetic field $\mathbf{H}$ created in the laboratory frame:

$$\mathbf{E}=\mathbf{E}'\gamma ,\quad \mathbf{H}=\frac{1}{c}\mathbf{v}\times\mathbf{E}. \tag{4}$$

Here $\mathbf{v}$ is the velocity of the pulse and the velocity of light is equal to $c=137.036$ in the system of units used.

Now let us evaluate the deflection angle θ_d of the particle in the external field (4) during the collision time $T=\gamma^{-1}L/2c$:

$$\theta_d=\frac{e}{p}\int_0^T E_\perp dt, \tag{5}$$

where p is the initial momentum of the projectile particle. The transverse field acting on the particle is equal to

$$\mathbf{E}_\perp=\mathbf{E}+\frac{1}{c}\mathbf{v}\times\mathbf{H}=2\gamma e\mathbf{E}'.$$

Substituting here the electric field $\mathbf{E}'$ from (3) we derive the result

$$\theta_d=\frac{Ne^2}{mc^2R}\gamma^{-1}=\frac{Ne^2}{mc^2R}\theta_r. \tag{6}$$

The factor Ne^2/Rmc^2 is equal to 1.4×10^2 for the SLC and 1.7×10^3 in the case of the supercollider. For the JLC this factor is 2.2×10^3. These estimates demonstrate that the deflection angle of the projectile particle in the pulse field surpasses substantially the radiation angle $\theta_r=1/\gamma$ in all cases under consideration. This result means that radiation in a certain direction is emitted only from a small piece of the particle trajectory, which can be approximated by a part of a circle. The external field of the pulse is nearly perpendicular to the direction of the particle's velocity. These conditions make the beamstrahlung problem similar to the problem of synchrotron radiation, which is treated for ultrarelativistic particles quasiclassically [3,4].

Let us prove that the quasiclassical condition is fulfilled in the problem considered. The quasiclassical approach is applicable if the de Broglie wavelength of a particle is substantially less than the length scale of a potential [9]. The length scale of the transverse potential of the pulse is of the order of R. The transverse de Broglie wavelength may be estimated as

$$\lambda \sim \frac{2\pi}{p_\perp} \sim \frac{2\pi}{(2m_0U_0)^{1/2}}\frac{1}{\gamma} \ll R \ , \tag{7}$$

where the perpendicular transferred momentum $p_\perp$ is taken from the relation

$$p_\perp^2/2m \sim U.$$

The potential depth U and the electron mass m in the laboratory frame are

$$U=U_0\gamma, \quad m=m_0\gamma \ .$$

Here U_0 and $m=m_0$ are the depth of the transverse potential and the mass of the electron in the pulse rest frame. The inequality (7) is fulfilled for ultrarelativistic particles ($\gamma \gg 1$) in all cases under consideration.

The totally classical treatment of the beamstrahlung process fails to describe correctly the particle energy loss in collision with the pulse. The classical theory considers the radiation of photons with frequencies much less than the particle energy. The fractional energy loss of the particle has to be small. It is described by the following expression [1]:

$$\delta_0=\frac{8N^2e^6}{3m^3c^6}\frac{\gamma^2}{LR^2} \ . \tag{8}$$

The classical approximation is therefore applicable for the SLC when $\delta_0 \sim 1.49\times 10^{-2} \ll 1$. For the supercollider δ_0 is $\sim 7.15\times 10^5 \gg 1$ and for JLC $\delta_0 \sim 1.13\times 10^2 \gg 1$. The large fractional energy loss appears due to predominance of the high-energy photons in the emitted spectrum. The quantum behavior of the radiation process manifests itself if the photon energy is comparable with the projectile energy. The performed estimate of δ_0 shows that the quantum corrections are very important and have to be considered in the beamstrahlung treatment.

III. QUASICLASSICAL DESCRIPTION OF THE BEAMSTRAHLUNG SPECTRUM

The spectrum of radiated frequencies of the electron moving along the circle trajectory in the uniform magnetic field is very well known. The quasiclassical consideration of this problem (see, e.g., [3,4]) gives the following expression for the radiation intensity:

$$\frac{dI}{d\omega} = -\frac{e^2m^2\omega c^3}{\varepsilon^2}\left\{\int_\xi^\infty \mathrm{Ai}(z)dz + \left[\frac{2}{\xi}+\frac{\omega}{\varepsilon}\chi\xi^{1/2}\right]\mathrm{Ai}'(x)\right\} , \tag{9}$$

$$\varepsilon=\varepsilon'+\omega, \quad \xi=\left[\frac{\omega}{\varepsilon'\chi}\right]^{2/3}, \quad \chi=\frac{\omega_0}{\varepsilon}\left[\frac{\varepsilon}{mc^2}\right]^3 .$$

The parameter ω_0 is defined as

$$\omega_0=\frac{c|e|H}{\varepsilon} ,$$

where H is the strength of the uniform magnetic field acting on the electron. The Airy function $\mathrm{Ai}(x)$ is introduced according to the definition

$$\mathrm{Ai}(x)=\frac{1}{\sqrt{\pi}}\int_0^\infty \cos(ux+u^3/3)du \ .$$

The expression (9) takes into account the main quantum corrections to the result of the classical theory [10] which follows from (9) in the limit of low frequencies $\omega/\varepsilon \to 0$. The physical origins of these corrections are the electron recoil during the emission of photons and the quantum motion of electron. The result (9) is applicable in the region of high photon frequencies $\omega \sim \varepsilon$ but not too close to the spectrum edge. The electron in the final state should still have an ultrarelativistic energy $\varepsilon' \gg mc^2$.

The analysis made in the preceding section shows that the electron radiates at any moment as in the synchrotron radiation process. Therefore, using the result (9), we obtain the spectral distribution of the total energy loss for an electron crossing the pulse as

$$\frac{d\varepsilon}{d\omega}=\int_0^T dt\frac{dI}{d\omega}(t) , \tag{10}$$

where $T=\gamma^{-1}L/2c$ is the time of the collision. The radiation intensity (9) depends on time because we take it at the position of the particle at any moment of time. Instead of the uniform magnetic field H appearing in (9) we substitute the transverse electric field $E_\perp$ [(see (5)] acting on the particle during the collision. The spectra distribution (10) depends on the chosen particle trajectory. In real experiments one cannot measure the radiation coming from a single particular trajectory, therefore the spectrum (10) has to be averaged over all possible trajectories of the electron. Considering only head-on collisions and using the axial symmetry of the pulse we obtain the following averaged photon distribution:

$$\left\langle\frac{d\varepsilon}{d\omega}\right\rangle=\frac{1}{R^2}\int_0^R \frac{d\varepsilon}{d\omega}d\rho^2 \ . \tag{11}$$

Introducing the ratio $y=\rho/R$ as a new variable and substituting (9) and (10) in (11), we derive the expression

$$\left\langle\frac{d\varepsilon}{d\omega}\right\rangle=-\frac{2e^2m^2\omega c^3}{\varepsilon^2}\times\int_0^1 dy\, y\int_0^T dt\left\{\int_z^\infty \mathrm{Ai}(\xi)d\xi+\left[\frac{2}{x}+\frac{\omega}{\varepsilon}\chi x^{1/2}\right]\mathrm{Ai}'(x)\right\} \tag{12}$$

where the parameters are defined as follows:

$$x=(\eta/\chi)^{2/3},\quad \eta=\omega/(\varepsilon-\omega),\quad \varepsilon=mc^2\gamma\ ,$$

$$\chi=\frac{eE_\perp\gamma}{m^2c^3},\quad \mathbf{E}_\perp=2\gamma\mathbf{E}'_\perp\ .$$

The electric field $\mathbf{E}'_\perp$ is taken from (3); $E_\perp$ is the transverse field acting on the particle in the laboratory frame.

The trajectory of the particle in the field of the pulse may be written as

$$r(t)=\rho[1+\nu(t)]\ , \tag{13}$$

where parameter ρ is the initial impact parameter and $\nu(t)$ characterizes deviation of the particle from ρ in the pulse field at time t. The maximum deviation is

$$\nu_{\max}\sim\frac{L\theta_d}{\rho}\ . \tag{14}$$

Here θ_d is the deflection angle of the electron estimated in (6).

Substituting in (14) the figures of Table I, we find that $\nu_{\max}=0.25$ for SLC and $\nu_{\max}=2\times10^{-2}$ for the supercollider. These estimates show that one can neglect this parameter in (13). The accuracy of this approximation is different for different cases.

Neglecting ν in (13) and substituting ρ instead of $r(t)$ in (12), one can perform easily the integration over time. The result reads

$$\left\langle\frac{d\varepsilon}{d\omega}\right\rangle=-\frac{e^2\gamma^{-3}\omega L}{c^2}\times\int_0^1 dy\, y\left\{\int_\xi^\infty \mathrm{Ai}(z)dz+\left[\frac{2}{z}+\frac{\omega}{\varepsilon}\chi z^{1/2}\right]\mathrm{Ai}'(z)\right\}. \tag{15}$$

To compare this result with the spectrum obtained in [1] we introduce another variable: the scaling parameter, which is a complicated combination of quantities characterizing the process,

$$C_b=\frac{m^2c^3RL}{4Ne^2\gamma^2}\ ,$$

and the ratio x, being convenient for the description of the spectral distribution of photons,

$$x=\frac{\varepsilon'}{\varepsilon},\quad 1-x=\frac{\omega}{\varepsilon}\ .$$

In the new variables the spectrum (15) reads

$$\left\langle\frac{d\varepsilon}{d\omega}\right\rangle=\delta_0(2x)C_bR(x;C_b)\ . \tag{16}$$

Here δ_0 is the classical fractional energy loss introduced in (8). The function $R(x;C_b)$ is equal to

$$R(x;C_b)=-3U^{3/2}\int_0^1 dy\, y\left\{\int_\xi^\infty \mathrm{Ai}(z)dz+\left[\frac{2}{\xi}+\frac{\omega}{\varepsilon}\chi\xi^{1/2}\right]\mathrm{Ai}'(\xi)\right\}. \tag{17}$$

The relations for the parameters here are

$$\xi=\frac{U}{y^{2/3}},\quad \chi=\frac{y}{C_b},\quad U=C_b^{2/3}\left[\frac{1-x}{x}\right]^{2/3}.$$

The expression for the function $R(x;C_b)$ can be simplified. Changing the integration order in the double integral in (17) and doing integration over y analytically (see Appendix A), we come to the final result, which we present in the form of the fractional energy loss

$$\frac{d\delta}{dx}=\left\langle\frac{d\varepsilon}{d\omega}\right\rangle. \tag{18}$$

Then the relation (16) reads

$$\frac{1}{C_b\delta_0}\frac{d\delta}{dx^2}=R(x;C_b)\ . \tag{19}$$

Here the function $R(x;C_b)$ is equal to

$$R(x;C_b)=R_1(U)+T(x)R_2(U)\ , \tag{20}$$

with

$$R_1(U)=-\tfrac{3}{2}U^{3/2}\int_U^\infty dz\ \mathrm{Ai}(z)\left[1-\frac{U^3}{z^3}\right],$$

$$R_2(U)=-9\int_U^\infty\frac{dz}{z^5}\mathrm{Ai}'(z)\ , \tag{21}$$

$$T(x)=\frac{x^2+1}{2x}\ .$$

The parameter U in these expressions is the same as in (17). The formulas (19)–(21) describe the scaling behavior of the beamstrahlung spectrum. This result differs from that derived in the purely quantum-mechanical treatment of the beamstrahlung process [1]. The result of paper [1] has the structure.

$$\frac{1}{C_b\delta_0}\frac{d\delta}{dx^2}=R(U)T(x)\ , \tag{22}$$

where the function $T(x)$ is the same as in (21) but the scaling function $R(U)$ differs from $R_1(U)$ and $R_2(U)$. Figure 1 presents the comparison of the functions $R_1(U)$ and $R_2(U)$ and $R(U)$.

Figure 2 shows the beamstrahlung spectra in different

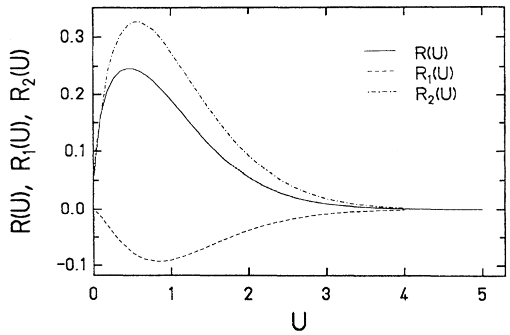

FIG. 1. Comparison of the scaling functions $R_1(U)$ and $R_2(U)$ with the function $R(U)$ of Ref. [1].

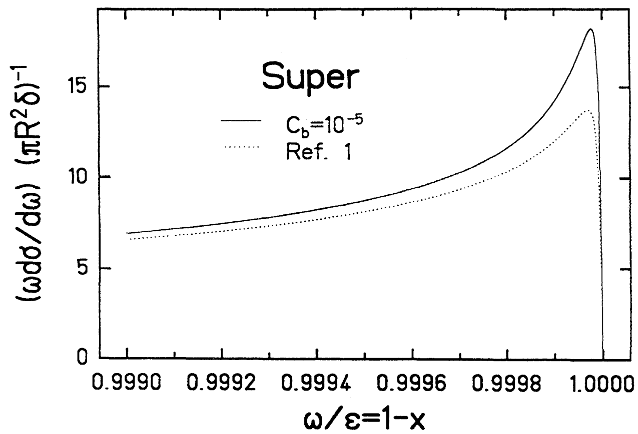

FIG. 3. The behavior of the beamstrahlung spectrum near the edge in the case of the supercollider.

cases. These spectra are normalized to the total radiation energy loss δ which we calculate in the next section. The maximum of the frequency distribution lies in the low-frequency region for SLC, while for the supercollider a sharp maximum exists near the spectrum edge. These two different kinds of behavior correspond to the classical and to the quantum limit of the beamstrahlung process. We also present the photon spectrum for an intermediate case. The classical limit corresponds to the large values of the scaling parameter C_b. On the contrary, this parameter is small in the quantum limit.

Figure 2 demonstrates the good agreement between the quantum [1] and the quasiclassical methods. That proves that the nature of the beamstrahlung process is described correctly as quasiclassical.

The peculiar behavior of the spectrum near the edge in the supercollider case is plotted in Fig. 3. This is the region where the discrepancy between the quasiclassical and the quantum methods is especially large. Indeed, the parameter x is small in this region ($x \ll 1$). Therefore the function $T(x)$ is large [$T(x) \gg 1$] and the corresponding term dominates in the $R(x;C_b)$. The spectrum (19), can be approximately expressed in the form (22) with the function $R_2(U)$ instead of $R(U)$. The difference between $R_2(U)$ and $R(U)$ is clear from Fig. 1. This discrepancy manifests itself in the corresponding spectral distributions of photons as plotted in Fig. 3. In the frequency region far from the spectrum edge the agreement between the results of the two methods is very good because of $T(x) \approx 1$ and $R(U) \approx R_1(U) + R_2(U)$.

Figure 4 shows the beamstrahlung spectra which are relevant to the three options of the JLC project (see Table I). The maximum in the frequency distribution appears here also near the edge, but it is not so sharp as in the case of the supercollider.

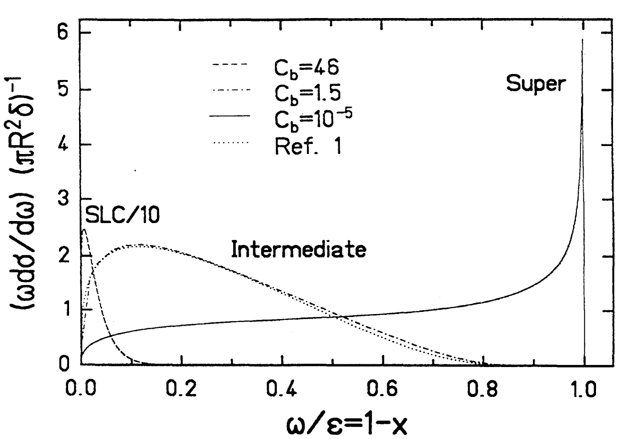

FIG. 2. The beamstrahlung spectra for different colliders.

IV. TOTAL ENERGY LOSS

To calculate the total beamstrahlung energy loss in the collision of an electron with a positron pulse we need to integrate the spectral distribution (15) over all photon frequencies. It is convenient to characterize the radiation process by the fractional energy loss which is defined as

$$\delta = \frac{1}{\varepsilon} \int_0^{\varepsilon} d\omega \left\langle \frac{d\varepsilon}{d\omega} \right\rangle . \tag{23}$$

This quantity is equal to δ_0—(8) in the classical limit. The function describing the deviation of the fractional energy loss from the classical result is called the form factor of the beamstrahlung process. Substituting (15) in

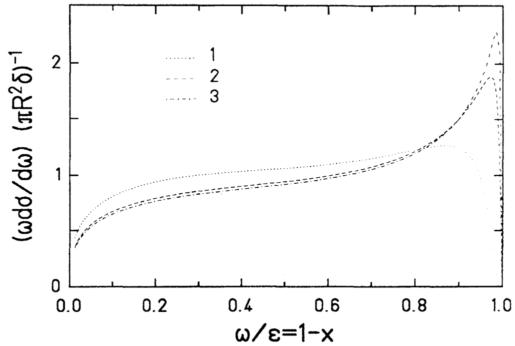

FIG. 4. The beamstrahlung spectra for the JLC project.

(23), we come to the following expression for the form factor:

$$F(C_b)=-\frac{e^2\gamma^{-4}L}{mc^4\delta_0}\int_0^1 dy\, y\int_0^\varepsilon d\omega\,\omega\left\{\int_\xi^\infty \mathrm{Ai}(z)dz+\left[\frac{2}{\xi}+\frac{\omega}{\varepsilon}\chi\xi^{1/2}\right]\times\mathrm{Ai}'(\xi)\right\} . \quad (24)$$

Changing the order of integration for ω and z and using ξ instead of ω as a new variable, we derive the result (see Appendix B)

$$F(C_b)=-3\int_0^1 dy\, y^3\int_0^\infty dx\, x\,\mathrm{Ai}'(x)\times\frac{4+5C_b^{-1}yx^{3/2}+4C_b^{-2}y^2x^3}{(1+C_b^{-1}yx^{3/2})^4} . \quad (25)$$

The expression (25) can be further simplified by changing the order of integration and integrating analytically over y. The result of the calculation is

$$F(C_b)=-3\int_0^\infty dx\, x\,\mathrm{Ai}'(x)\times\left\{\frac{24}{y_0}\ln(1+y_0)+\frac{2y_0^4-5y_0^3-44y_0^2-60y_0-24}{y_0^3(1+y_0)^3}\right\} . \quad (26)$$

The parameter y_0 in (26) is defined as

$$y_0=\frac{1}{C_b}x^{3/2} .$$

Using (26) we can easily investigate the behavior of the form factor both in the classical and in the quantum limits. The expansion of (26) in the region of large scaling parameters $C_b \gg 1$ results in

$$F(C_b)\approx 1-\frac{11\sqrt{3}}{4C_b}+\frac{96}{3C_b^2}+\cdots , \quad C_b\gg 1 . \quad (27)$$

The expansion of (26) in the region of small parameters C_b shows the following behavior:

$$F(C_b)\approx\alpha_0 C_b^{4/3}\{1+\alpha_1 C_b^{2/3}+\alpha_2 C_b^{4/3}+\cdots\} , \quad C_b\ll 1 . \quad (28)$$

The expressions for the coefficients α_i in (28) are

$$\alpha_0=2^3\times 3^{-7/3}\Gamma(\tfrac{2}{3})\approx 0.833 ,$$

$$\alpha_1=-2^{-2}\times 3^{7/3}\Gamma^{-1}(\tfrac{2}{3})=-2\alpha_0^{-1}\approx -2.4 ,$$

$$\alpha_2=2^{-3}\times 3^{-1/3}(55)\Gamma(\tfrac{1}{3})\Gamma^{-1}(\tfrac{2}{3})\approx 9.4 ,$$

where $\Gamma(\frac{1}{3})\approx 2.6789$ and $\Gamma(\frac{2}{3})\approx 1.3541$.

The numerical fit of the coefficients α_0, α_1 in the limiting formulas for $F(C_b)$, being made in [1], is in a good agreement with our results. According to [1], $\alpha_0\approx 0.83$ and $\alpha_1\approx -2.0$.

The result of integration over x in (25) can be expressed as a power series in the region of small and large parameters C_b. Then, the integration over y becomes trivial. The analysis of the similar integral is given in [4] and therefore we present here only the final result of this calculation,

$$F(C_b)=\frac{3\sqrt{3}}{16\pi}\sum_{k=0}^{\infty}(-1)^k\frac{4(k+1)}{k+4}(k^2+2k+8)\Gamma\left[\frac{k}{2}+\frac{2}{3}\right]\Gamma\left[\frac{k}{2}+\frac{4}{3}\right]\left[\frac{3}{C_b}\right]^k , \quad C_b\gg 1 , \quad (29)$$

$$F(C_b)=3\sqrt{3}\pi\sum_{k=0}^{\infty}\left\{\frac{4(6k+1)(9k^2+3k+16)}{27k!(4-3k)\Gamma(k+\frac{1}{3})}\left[\frac{C_b}{3}\right]^{2k+4/3}+\frac{4(6k+5)(9k^2+15k+22)}{27k!(2-3k)\Gamma(k+\frac{5}{3})}\left[\frac{C_b}{3}\right]^{2k+8/3}-\frac{k(k^2+7)}{[2-(-1)^k](3-k)\Gamma(k/2+\frac{1}{6})\Gamma(k/2+\frac{5}{6})}\left[\frac{C_b}{3}\right]^{k+1}\right\} , \quad C_b\ll 1 . \quad (30)$$

The series (29) and (30) has the asymptotical convergence. Therefore these formulas can be used only if the corresponding conditions on C_b are well fulfilled.

The result of numerical calculation of the beamstrahlung form factor (25) and (26) is shown in Fig. 5. The form factor tends to unity in the classical limit, where the parameter C_b is large. In the quantum limit the form factor goes to zero. This limit corresponds to the region of small parameters C_b. Figure 5 shows as well the comparison of our result with the form factor obtained in [1]. It is clear from Fig. 5 that the discrepancy between the predictions of the two methods is less than a few percent.

Having the form factor $F(C_b)$ one can easily derive the fractional energy loss in the following manner:

$$\delta=\delta_0 F(C_b) . \quad (31)$$

Calculating the form factor which is appropriate to the

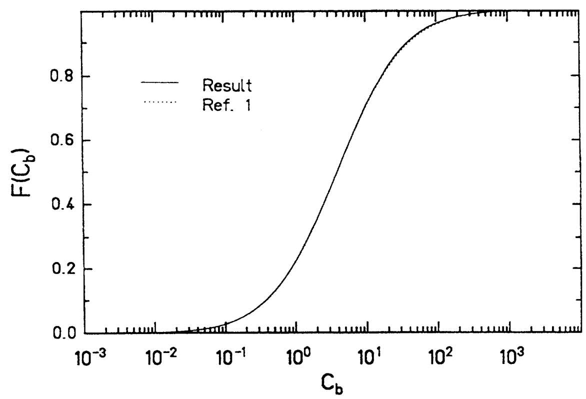

FIG. 5. The form factor of the beamstrahlung process.

SLC and supercollider, we come to the following energy losses:

$$\delta_{\rm SLC}=0.014,\quad C_b=46\ ,$$
$$\delta_{\rm super}=0.17,\quad C_b=10^{-5}\ . \tag{32}$$

The quasiclassical treatment provides the fractional energy loss, which is substantially suppressed in comparison with the classical result in cases pertaining to the quantum scenario of the process.

V. CONCLUSION

We have described the beamstrahlung process by the quasiclassical method. We have calculated the frequency distribution of the emitted photons and the radiation energy loss. The quantum behavior of the electron in the beamstrahlung process results in considerable suppression of the radiation intensity in comparison with the predictions of the classical theory. Another specific feature of the beamstrahlung process in the quantum scenario is the appearance of a sharp maximum in the photon frequency distribution near the edge of the spectrum. This kind of behavior differs from a dependence characterizing the classical case. In the classical limit a broad maximum appears in the low-frequency region.

We have compared the results of our numerical calculations with the predictions of a quantum-mechanical treatment of the beamstrahlung and found a good agreement of the two different approaches. However, the form of the scaling law is different. This discrepancy manifests itself especially strongly in the region of large frequencies near the spectrum edge but influences the total energy loss only weakly.

We confirmed a relatively large fractional energy loss for envisaged TeV colliders.

The accuracy of the method may be improved by a more precise description of the particle trajectory in the pulse. It might be important for denser pulses when the deflection of the electron is considerable.

Let us note that our method is also appropriate for the description of the channeling radiation as well as for the description of pair creation process by photons in the field of a pulse or an oriented monocrystal. All these processes are very similar in nature and the quasiclassical approach offers a very efficient and reliable way to describe them.

ACKNOWLEDGMENTS

We are thankful to W. Greiner for his interest and critical comments on our work. This work was supported by Alexander von Humbolt Stiftung.

APPENDIX A

Let us perform the transformation of the function $R(x;C_b)$, (17), which was used in (19)–(21). Using $\xi=y^{-2/3}U$ instead of y as the new integration variable, we derive

$$R(x;C_b)=-\tfrac{9}{2}U^{9/2}\int_U^\infty\frac{d\xi}{\xi^4}\left\{\int_\xi^\infty {\rm Ai}(z)dz+\frac{1+x^2}{x}\frac{{\rm Ai}'(\xi)}{\xi}\right\}.$$

This function can be represented as

$$R(x;C_b)=R_1(U)+T(x)R_2(U)\ ,$$

where the functions $R_1(U)$ and $R_2(U)$ are defined as

$$R_1(U)=-\tfrac{9}{2}U^{9/2}\int_U^\infty\frac{d\xi}{\xi^4}\int_\xi^\infty dz\,{\rm Ai}(z)\ ,$$

$$R_2(U)=-9U^{9/2}\int_U^\infty\frac{d\xi}{\xi^5}{\rm Ai}'(\xi)\ .$$

Changing the order of integration in $R_1(U)$ and doing afterwards the integration over ξ we come to the result

$$R_1(U)=-\tfrac{3}{2}U^{3/2}\int_U^\infty d\xi\,{\rm Ai}(\xi)\left[1-\frac{U^3}{\xi^3}\right].$$

APPENDIX B

Here we present the transformation of the double integral, which appeared in (24),

$$I=\int_0^\varepsilon d\omega\,\omega\left\{\int_z^\infty{\rm Ai}(\xi)d\xi+\left[\frac{2}{x}+\frac{\omega}{\varepsilon}\chi x^{1/2}\right]{\rm Ai}'(x)\right\}.$$

Introducing the new integration variable x instead of ω and using the relation

$$\omega=\varepsilon\left[1-\frac{1}{1+C_b^{-1}yx^{3/2}}\right],$$

we derive the result

$$I=I_1+I_2\ ,$$

where the contributions I_1 and I_2 are

$$I_1=\frac{3}{2}\frac{\varepsilon^2y^2}{C_b^2}\int_0^\infty dx\frac{x}{(1+C_b^{-1}yx^{3/2})^4}\times(2+2C_b^{-1}yx^{3/2}+C_b^{-2}y^2x^3){\rm Ai}'(x)\ ,$$

$$I_2=\frac{3}{2}\frac{\varepsilon^2 y}{C_b}\int_0^\infty dx\frac{x^{1/2}}{(1+C_b^{-1}yx^{3/2})^2}\left[1-\frac{1}{1+C_b^{-1}yx^{3/2}}\right]\times\int_x^\infty dx'\,\mathrm{Ai}(x') .$$

Changing the integration order in the double integral I_2 and integrating over x, we obtain

$$I_2=\frac{\varepsilon^2 y^2}{2C_b^2}\int_0^\infty dx\ \mathrm{Ai}(x)\frac{x^3}{(1+C_b^{-1}yx^{3/2})^2} .$$

Using the relation

$$\mathrm{Ai}(x)=\frac{1}{x}\mathrm{Ai}''(x)$$

and integrating I_2 by parts, we come to the result

$$I_2=-\frac{\varepsilon^2 y^2}{2C_b^2}\int_0^\infty dx\frac{\mathrm{Ai}'(x)}{(1+C_b^{-1}yx^{3/2})^4}x(2-C_b^{-1}yx^{3/2})\times(1+C_b^{-1}yx^{3/2}) .$$

Substituting I_1 and I_2 in I, we derive the final result

$$I=\frac{\varepsilon^2 y^2}{2C_b^2}\int_0^\infty dx\ x\ \mathrm{Ai}'(x)\frac{4+5C_b^{-1}yx^{3/2}+4C_b^{-2}y^2x^3}{(1+C_b^{-1}yx^{3/2})^4} .$$

---

*Permanent address: A. F. Ioffe Physical-Technical Institute of the Academy of Sciences of Russia, 194021 St. Petersburg, Russia.

[1] R. Blankenbecler and S. D. Drell, Phys. Rev. D **36**, 277 (1987).
[2] M. Jacob and T. T. Wu, Nucl. Phys. B **303**, 273 (1988); **303**, 389 (1988).
[3] L. D. Landau and E. M. Lifshitz, *Quantum Electrodynamics* (Pergamon, London, 1965).
[4] V. N. Bayer, V. M. Katkov, and V. M. Strahovenko, *High Energy Electromagnetic Processes in Oriented Monocrystals, Novosibirsk* (Nauka, Moscow, 1989).
[5] R. Blankenbecler and S. D. Drell, Phys. Rev. Lett. **61**, 2324 (1988).
[6] M. Jacob and T. T. Wu, Nucl. Phys. B **314**, 334 (1989).
[7] M. Jacob and T. T. Wu, Nucl. Phys. B **318**, 53 (1989).
[8] S. Takeda, *Present Status of R&D for JLC Project,* in Proceedings of the Second Workshop on Japan Linear Collider (JLC) [National Laboratory for High Energy Physics (KEK), Ibaraki, Japan, 1990], Vol. 318, pp. 6 and 53.
[9] L. D. Landau and E. M. Lifshitz, *Quantum Mechanics* (Pergamon, London, 1965).
[10] L. D. Landau and E. M. Lifshitz, *Classical Theory of Fields* (Pergamon, London, 1961).